

Frequency-Resolved Optical Gating Using Cascaded Second-Order Nonlinearities

Alfred Kwok, Leonard Jusinski, Marco A. Krumbügel, John N. Sweetser,
David N. Fittinghoff, and Rick Trebino

(*Invited Paper*)

Abstract— We demonstrate frequency-resolved optical gating (FROG) using cascaded second-order nonlinearities (up-conversion followed by down-conversion). We describe two different cascaded second-order beam geometries—self-diffraction and polarization-gate—which are identical to their third-order nonlinear-optical cousins, except that they use second-harmonic-generation crystals instead of (weaker) third-order materials. Like the corresponding third-order processes, these new versions of FROG yield the same intuitive traces, uniquely determine the pulse intensity and phase (without direction-of-time ambiguity), and yield signal light at the input-pulse wavelength (which simplifies the required spectral measurements). Most importantly, however, we show that these techniques are significantly more sensitive than the corresponding third-order FROG methods, conveniently allowing, for the first time, the unambiguous measurement of ultrashort $\sim 1\text{-nJ}$ pulses, that is, unamplified Ti:sapphire oscillator pulses.

Index Terms— Femtosecond, frequency-resolved optical gating (FROG), ultrafast.

I. AMPLIFIED VERSUS UNAMPLIFIED ULTRASHORT-LASER-PULSE MEASUREMENT

THE RECENT development of techniques for measuring the intensity and phase of ultrashort-laser pulses has benefitted amplified ($>\mu\text{J}$) pulses more than unamplified ($\sim\text{nJ}$) pulses. For amplified-pulse measurement, the most commonly used method, frequency-resolved optical gating (FROG) [1]–[4], typically uses third-order nonlinear-optical processes, which generate highly intuitive spectrograms and yield unambiguous measurements. Third-order processes are not strong enough to allow FROG measurements of unamplified pulses, however. As a result, FROG measurements of unamplified pulses require the use of a second-order process, that is, second-harmonic generation (SHG), to obtain sufficient sensitivity [3]. While it has some advantages, SHG FROG unfortunately yields unintuitive traces (See Fig. 1) and direction-of-time ambiguity. Unlike third-order methods, it involves detection at the second harmonic of the input-pulse wavelength (usually the UV), where wavelength-dependent responses in optics, spectrometers, and detectors are more likely to bias the measurement. As a result, the measurement

Manuscript received November 20, 1997; revised March 23, 1998. This work was supported by the U.S. Department of Energy, Basic Energy Sciences, Chemical Sciences Division.

The authors are with the Combustion Research Facility, Sandia National Laboratories, Livermore, CA 94550 USA.

Publisher Item Identifier S 1077-260X(98)04188-4.

of unamplified pulses is less convenient and more susceptible to error than the measurement of amplified pulses.

The use of the surprisingly strong surface third-harmonic-generation (THG) [5] effect attains sufficient sensitivity to measure unamplified pulses (and it has succeeded in this endeavor), but it requires detection at an even shorter wavelength. And, while THG FROG lacks direction-of-time ambiguity, its traces are only slightly asymmetrical and hence not as intuitive as those of other third-order FROG methods. In addition, surface THG FROG requires overlapping beams focused to few-micrometer spots. While surface THG FROG appears useful for measuring extremely short pulses (due to its extremely short interaction length and hence large bandwidth), it is not quite as convenient as other third-order FROG methods.

In this paper, we propose and demonstrate a method that achieves all of the desired goals: intuitive traces, completely unambiguous intensity-and-phase measurement, signal light at the fundamental wavelength, and sufficient sensitivity to measure unamplified Ti:sapphire laser-oscillator pulses. It is FROG using cascaded $\mathcal{X}^{(2)}$ effects for the optical nonlinearity, specifically, up-conversion followed by down-conversion.

II. CASCADED SECOND-ORDER NONLINEARITIES

Cascaded $\mathcal{X}^{(2)}$ (CC) effects simulate third-order nonlinearities but are significantly stronger [6]–[8]. A number of applications requiring greater signal strength than is available from third-order materials have been proposed and demonstrated using CC effects. Typically, CC effects involve SHG of one beam, followed by a down-conversion process involving the newly created second harmonic and another beam at the fundamental frequency. The signal beam is then at the fundamental frequency. The two processes are typically not simultaneously phase-matched, but can be approximately phase-matched, yielding an overall efficiency that is approximately the square of the SHG efficiency. This efficiency can be considerably greater than that available from a single $\mathcal{X}^{(3)}$ effect.

We will show that simply by using a SHG FROG apparatus, where, instead of detecting the second-harmonic, we detect an additional “self-diffracted” beam that is simultaneously created but not usually considered (see Fig. 2), we can perform an effective third-order FROG measurement of a pulse. This additional beam was first studied by Danielius *et al.* [6] who showed that, in a two-beam geometry, SHG of the first beam can be followed by a down-conversion process involving that

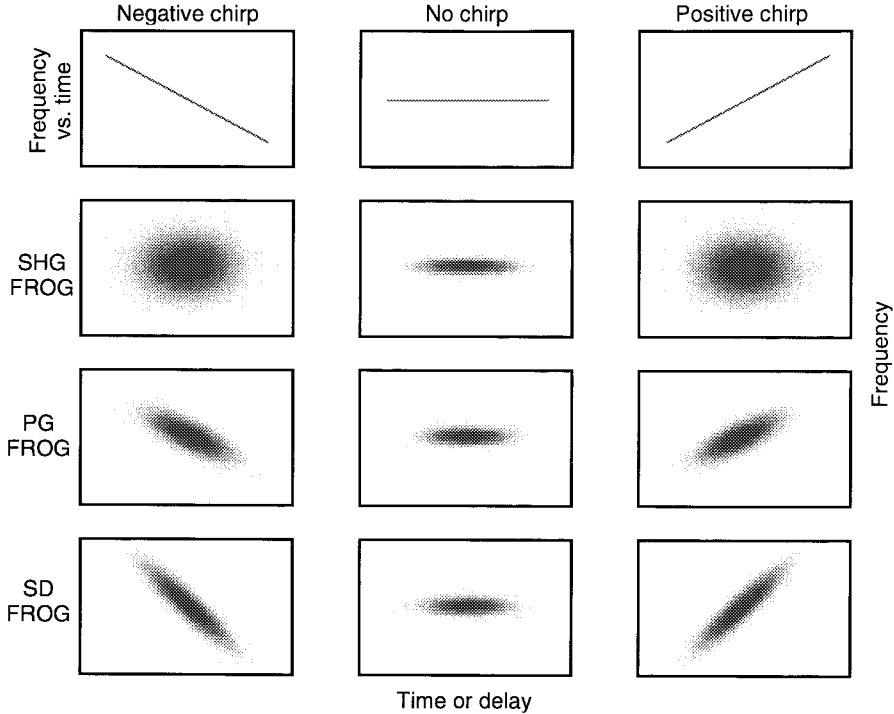


Fig. 1. Comparison of SHG, PG, and SD FROG traces for linearly chirped and unchirped pulses. Note that PG and SD FROG traces are tilted in accordance with the frequency-versus-time curve of the pulse (SD FROG traces are twice as sloped as PG FROG traces for linearly chirped pulses), while SHG FROG traces are not. It is this symmetry in SHG FROG traces that yields the ambiguity in the direction of time in SHG FROG measurements. (THG FROG traces for linearly chirped pulses are nearly identical to those of SHG FROG). CC FROG traces are identical to the intuitive SD or PG FROG traces, depending on the beam geometry chosen, and hence are free of ambiguity.

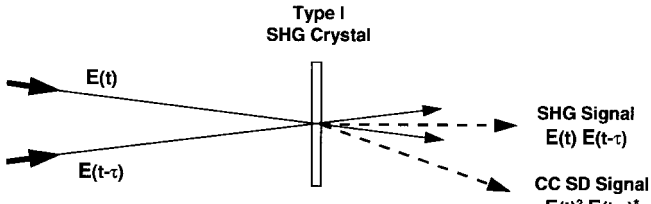


Fig. 2. Schematic diagram of cascaded $\chi^{(2)}$ self-diffraction FROG (CC SD FROG). In this process, the second harmonic of $E(t)$ combines in a down-conversion process with $E(t - \tau)$ to produce the "self-diffracted" beam of the form, $E(t)^2 E(t - \tau)^*$. Note also the SHG autocorrelation signal, $E(t)E(t - \tau)$, which is also produced and which can be used to make an SHG FROG trace simultaneously.

second-harmonic beam and the other fundamental input beam yielding an additional beam at the fundamental wavelength. This process is analogous to a third-order self-diffraction process because the signal beam propagates in the direction $2\mathbf{k}_1 - \mathbf{k}_2$, where \mathbf{k}_i is the i th beam k -vector. No induced grating occurs, as in the usual self-diffraction process, however. On the other hand, this CC process will occur if the third-order medium in a standard self-diffraction geometry is simply replaced with a SHG crystal.

Cascaded $\chi^{(2)}$ self-diffraction FROG (CC SD FROG) simply involves spectrally resolving this self-diffracted beam for a range of delays. Thus, a CC SD FROG apparatus can be created simply by replacing the third-order medium in a SD FROG apparatus by a SHG crystal. The analogy to SD FROG is a good one: CC SD FROG traces made in this manner are mathematically identical to those made using a true third-order

SD FROG beam geometry. As a result, they are quite intuitive, and, like SD FROG traces, they uniquely determine the pulse intensity and phase.

In this paper, we also consider a second CC FROG arrangement involving a polarization-gate (PG) beam geometry (see Fig. 3), and which we will call CC PG FROG. It simply involves replacing the usual optical-Kerr medium between the crossed polarizers in a standard optical-Kerr PG arrangement with a type-II SHG crystal. All other aspects of this geometry are identical to the usual PG arrangement. In a previous publication [7], we showed that this arrangement yields optical switching. Here, we spectrally resolve the signal pulse that passes through the crossed polarizers to produce a PG FROG device, precisely as in $\chi^{(3)}$ PG FROG devices. Again, the analogy to polarization gating is also valid: traces produced in this manner are identical to those of PG FROG using a true third-order medium. Use of a CC process, however, produces a device that is significantly more sensitive.

Both CC SD FROG and CC PG FROG (which we will collectively refer to as CC FROG) generate highly intuitive FROG spectrograms, yield unambiguous measurements, and involve detection at the input-pulse wavelength. And CC FROG is sufficiently sensitive that it can measure *unamplified* Ti:sapphire oscillator pulses. It is trivial to convert an SHG FROG or SD FROG to a CC SD FROG apparatus, and it is trivial to convert a PG FROG apparatus to a CC PG FROG apparatus. Because CC FROG traces are mathematically identical to highly intuitive SD or PG FROG traces (see Fig. 1), the standard FROG computer algorithm works without

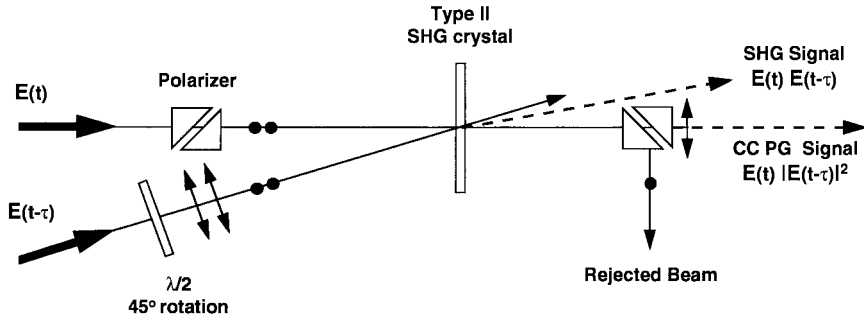


Fig. 3. Schematic diagram of cascaded $\chi^{(2)}$ polarization-gate FROG (CC PG FROG). Note the type-II SHG autocorrelation signal, $E(t)E(t - \tau)$, which is also produced and which can be used to make an SHG FROG trace simultaneously.

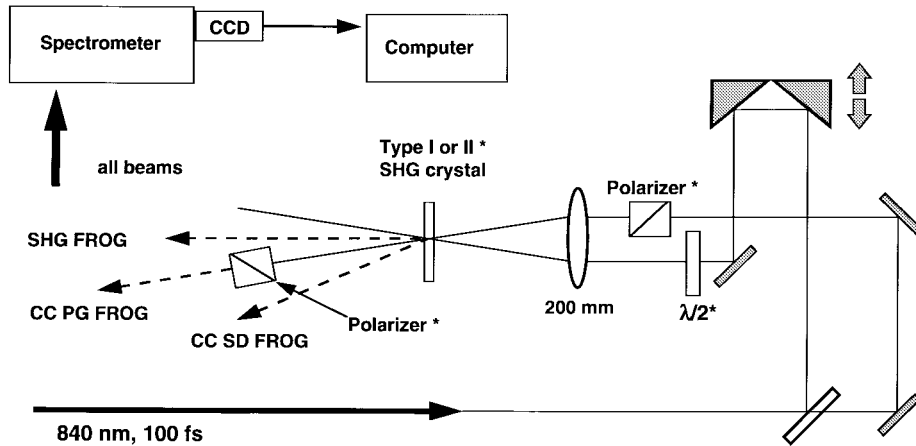


Fig. 4. Schematic diagram of CC SD and CC PG FROG apparatuses. The asterisked components (the polarizers, $\lambda/2$ waveplate, and type-II crystal) are required only for CC PG FROG and not for CC SD FROG measurements. For CC SD FROG measurements, a type-I or -II crystal was used. For CC PG FROG measurements, a type-II crystal is required. In both cases, a SHG FROG signal is simultaneously produced. The beam-steering optics leading to the spectrometer are not shown.

modification for CC FROG traces. Finally, a second-harmonic beam propagating between the two input pulses is necessarily simultaneously produced in both CC FROG apparatuses, so an SHG autocorrelation or SHG FROG trace can easily be obtained if corroboration is desired or if the laser intensity drops so that additional sensitivity is required.

III. SPECIFICS OF CC FROG

Consider first CC SD FROG. The second-harmonic field produced by a pulse, $E(t)$, is given by $E_{\text{SH}}(t) \propto E(t)^2$. If this field then acts in conjunction with a delayed replica of the pulse, $E(t - \tau)$, in a down-conversion process, as [6] has shown, the following field results:

$$E_{\text{CCSD}}(t, \tau) \propto E_{\text{SH}}(t)E^*(t - \tau) \quad (1)$$

Substituting for $E_{\text{SH}}(t)$, we have:

$$E_{\text{CCSD}}(t, \tau) \propto E^2(t)E^*(t - \tau). \quad (2)$$

This expression has the same dependence on the fields as self-diffraction, a third-order process. Indeed, also as in self-diffraction, the k -vector of this field is $\mathbf{k}_{\text{CC}} = 2\mathbf{k}_1 - \mathbf{k}_2$, where \mathbf{k}_1 and \mathbf{k}_2 are the k -vectors of $E(t)$ and $E(t - \tau)$, respectively. While the phase-matching properties of the two second-order processes involved are different, use of a small

beam angle (about a degree) maintains approximate phase-matching in both processes simultaneously. Typically, a type-I SHG crystal is used and therefore the polarizations of the two input beams are the same. This field is then spectrally resolved and detected with a slow energy detector, yielding a measured CC SD FROG signal of the form

$$I_{\text{CCSD}}(\omega, \tau) = \left| \int_{-\infty}^{\infty} E^2(t)E^*(t - \tau) \exp(-i\omega t) dt \right|^2. \quad (3)$$

It is important to note that a CC SD FROG measurement is also possible using a type-II crystal when one pulse is polarized at 45° relative to the other since, in this case, type-II SHG of $E(t)$ is created, which then interacts with $E(t - \tau)$ (via down-conversion) to generate the type-II SD signal. However, because it uses the usually smaller effective nonlinearity associated with type-II processes, and due to the dependence [7] of the CC signal strength on the fourth power of $\chi^{(2)}$, it is generally preferable to use the stronger type-I process for CC SD FROG measurements of relatively weak pulses.

We now consider CC PG FROG. Fig. 3 shows a schematic of the two processes that contribute to this effect. First, a type-II SHG crystal is placed between the two polarizers with its principal axes parallel and perpendicular to those of the polarizers (and so does not introduce additional leakage despite its birefringence). As in a standard polarization-gate

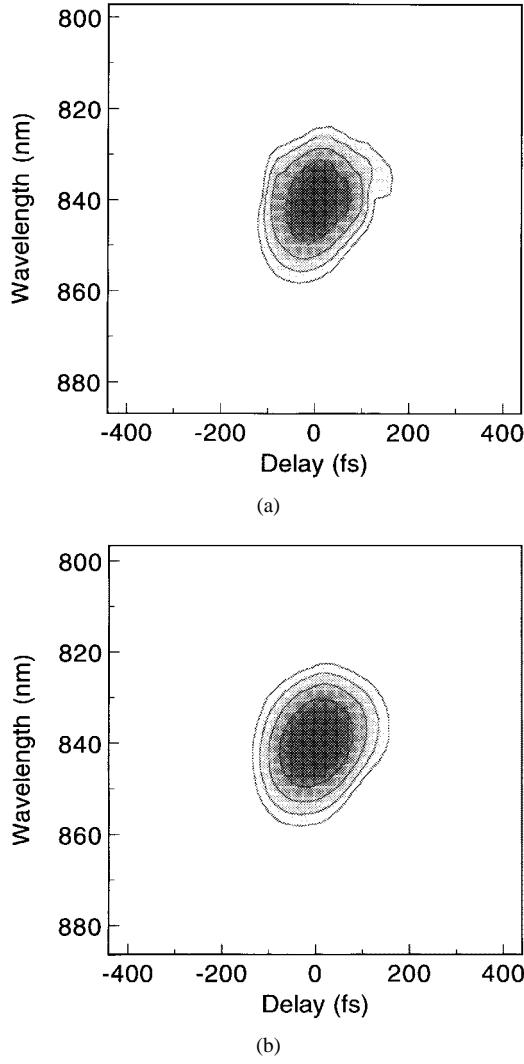


Fig. 5. Measured (a) and reconstructed (b) CC SD FROG trace of the oscillator pulse train. (Contour lines in these and all other figures in this paper are at 5%, 10%, 20%, 40%, 60%, and 80% of the maximum intensity.)

apparatus, the beam passing through the crossed polarizers (the “probe” beam) is horizontally polarized, and the “gate” beam has both polarizations (and, ideally, is 45° linearly polarized or circularly polarized). In the first second-order process, the vertical polarization component of the gate beam, $E_v(t - \tau)$, combines with the horizontally polarized probe beam, $E(t)$, to produce phase-matched type-II second harmonic: $E_{\text{SH}}(t, \tau) \propto E(t)E_v(t - \tau)$. The second second-order process then involves this newly produced second harmonic, $E_{\text{SH}}(t, \tau)$, combining with the horizontally polarized component of the gate beam, $E_h(t - \tau)$, to produce vertically polarized light collinear with the probe beam and at the fundamental frequency. This vertically polarized light then passes through the polarizer and is the signal. This signal pulse field has the expression:

$$E_{\text{CCPG}}(t, \tau) \propto E_{\text{SH}}(t)E_h(t - \tau)^*. \quad (4)$$

Substituting for $E_{\text{SH}}(t, \tau)$, we have

$$E_{\text{CCPG}}(t, \tau) \propto E(t)E_v(t - \tau)E_h(t - \tau)^*. \quad (5)$$

But both polarization components of the gate pulse are

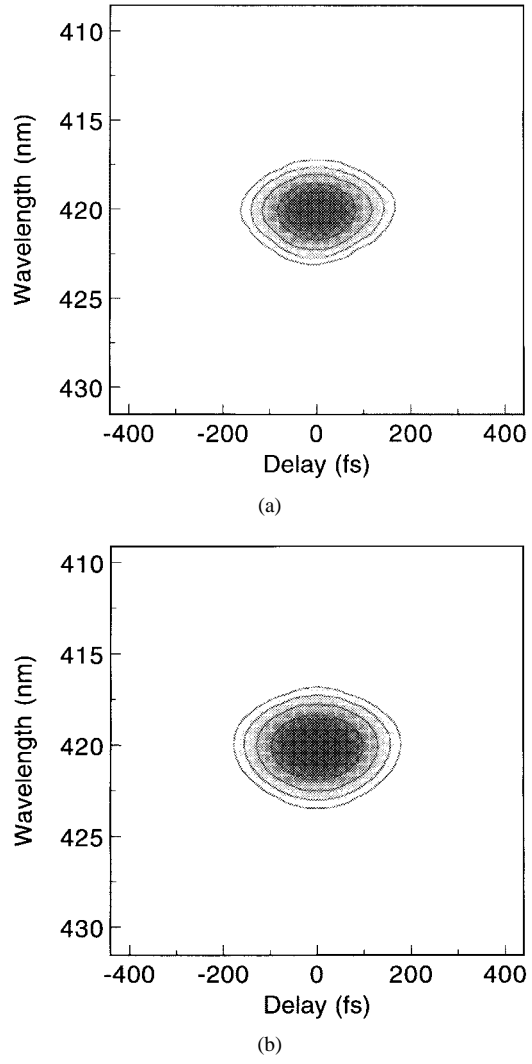


Fig. 6. Measured (a) and reconstructed (b) SHG FROG traces of the same oscillator pulse train as in the previous figure.

identical, so $E_v(t - \tau) = E_h(t - \tau) \equiv E(t - \tau)$. Thus, we have

$$E_{\text{CCPG}}(t, \tau) \propto E(t)|E(t - \tau)|^2 \quad (6)$$

which is the same expression as for the usual (third-order) PG FROG signal field. Thus, the corresponding CC PG FROG trace is

$$I_{\text{CCPG}}(\omega, \tau) = \left| \int_{-\infty}^{\infty} E(t)|E(t - \tau)|^2 \exp(-i\omega t) dt \right|^2. \quad (7)$$

Unlike the CC SD process described above, this CC PG process is completely phase-matched. As long as the crystal’s extraordinary polarization axis is perpendicular to the plane of the beams, both extraordinary rays have the same refractive index, and, if one process is phase-matched, the other process is also necessarily phase-matched, independent of the angle between the probe and gate beams.

We can estimate the nonlinear-optical efficiency of these processes. We first note that (assuming at least approximate phase-matching) the efficiency of the down-conversion process is about the same as that of the SHG process. So the overall

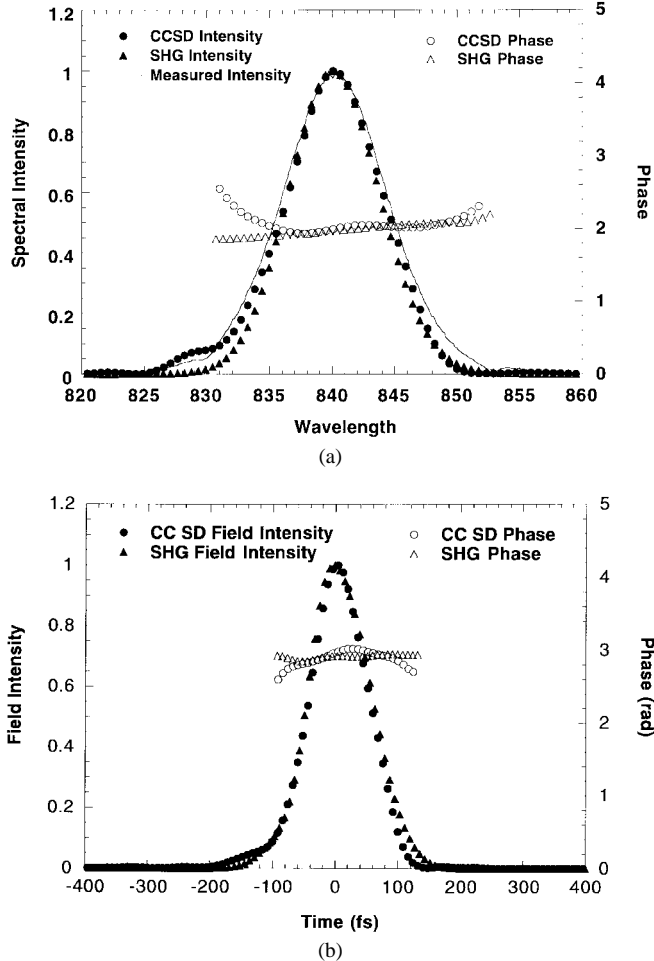


Fig. 7. (a) Retrieved electric field spectral intensities and phases versus wavelength for the FROG traces shown in Figs. 5 and 6. The standard SD FROG algorithm was used to retrieve the pulse from the CC SD FROG trace. The independently measured spectrum is also shown for comparison. (b) Retrieved electric field intensities and phases versus time.

cascaded $\chi^{(2)}$ process efficiency is clearly approximately the square of the SHG efficiency. Since it is straightforward to achieve few-percent SHG efficiency with $\sim nJ$ 100-fs pulses typical of Ti:sapphire oscillators, we then expect $\sim 10^{-4}$ efficiency for the cascading of the two $\chi^{(2)}$ processes. Thus, we expect the efficiency of the overall process to be sufficient to achieve measurements of unamplified Ti:sapphire oscillator pulses.

IV. EXPERIMENTAL DETAILS

Our CC FROG apparatus (see Fig. 4) consisted of a continuous-wave (CW) mode-locked Ti:sapphire oscillator, emitting several-nJ pulses at a 10⁸-Hz repetition rate. This pulse train was split into two using a 50/50 beam splitter, one train was variably delayed with respect to the other, and the beams were then recombined at a 1-mm-thick type-I BBO crystal and focused with a 200-mm focal-length lens. The beam interaction angle external to the crystal, which must be kept small to approximately phase-match both cascaded processes in CC SD FROG measurements, was 1.5°. The crystal was aligned to yield collinear SHG of each individual beam and also noncollinear SHG involving both beams, thus

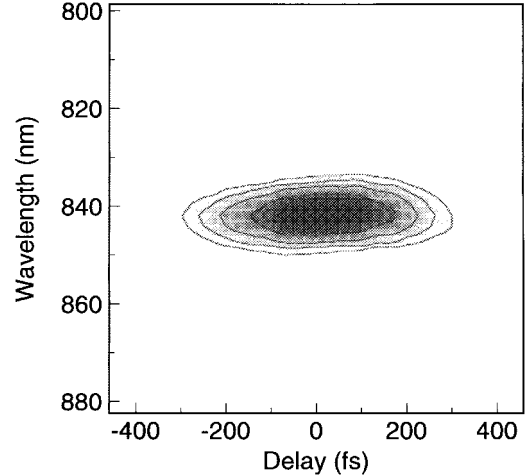


Fig. 8. Measured CC PG FROG trace of an attenuated amplified pulse train with about 100 nJ per pulse. As required, the standard PG FROG algorithm was used to retrieve the pulse from the CC PG FROG trace.

verifying, not only the phase-matching requirements, but also the beam overlap in time and space. This alignment then guarantees the existence of the CC SD beam, as well as the CC PG signal beam when polarizers and a type-II crystal are used. The signal beam (whether SD or PG) was then apertured and recollimated. The signal efficiency was approximately 10⁻⁴ in CC SD FROG measurements of the Ti:sapphire oscillator and about 10⁻³ in CC PG FROG measurements of attenuated regeneratively amplified pulses of about 100 nJ. The signal beam was spectrally resolved and detected using a 270-mm focal length, 600-line/mm grating Spex 270M imaging spectrometer and CCD camera (although we obtain similar results using a nonimaging or home-made spectrometer and inexpensive TV camera). We used considerable care to suppress scattered light from the input beams, which was of the same color and at nearly the same propagation direction as the signal beam.

V. EXPERIMENTAL RESULTS

A measured CC SD FROG trace of the oscillator pulse train is shown in Fig. 5. The standard SD FROG algorithm was used to retrieve the pulse from this trace. The retrieved trace is also shown in Fig. 5. The relative root-mean-square (rms) error between the measured and retrieved traces, a measure of the accuracy of the measurement, is 0.0086, which indicates a fairly accurate measurement [9], [10]. Visual agreement between the measured and retrieved traces is also good. In order to further check this measurement, we also made an SHG FROG measurement using the same apparatus and using the second-harmonic beam that is simultaneously produced (although the measurement was made later). The pulse intensity and phase were retrieved from this trace using the SHG FROG algorithm. The measured and retrieved SHG FROG traces are shown in Fig. 6. The relative rms error between the measured and retrieved SHG FROG traces is 0.010, which indicates a fairly accurate measurement [9], [10]. Visual agreement between the measured and retrieved SHG FROG traces is also good. The retrieved intensities and phases

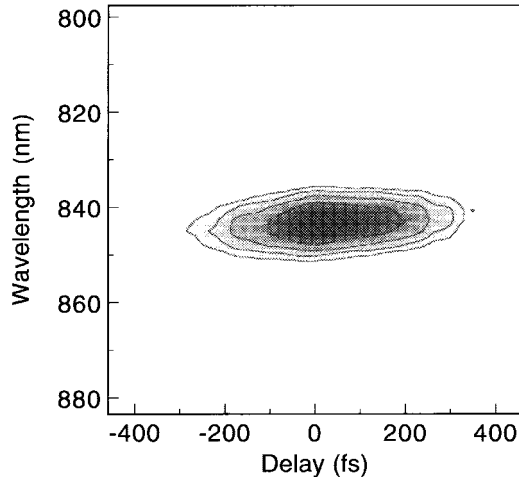


Fig. 9. Measured CC SD FROG trace (using a type-II crystal) of the same attenuated amplified pulse train (made for the purpose of checking the CC PG FROG pulse measurement shown in Fig. 8). As required, the standard SD FROG algorithm was used to retrieve the pulse from the CC SD FROG trace.

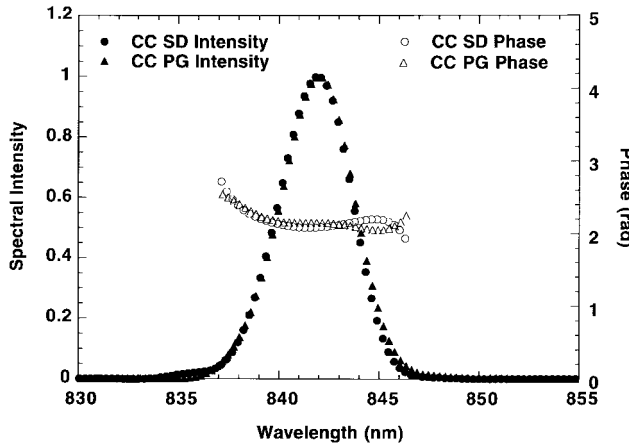


Fig. 10. Retrieved spectral intensities and phases vs. wavelength of the CC PG and CC SD FROG traces shown in Figs. 8 and 9. Note the good agreement between the two measurements.

are shown in Fig. 7, which also shows the independently measured pulse spectrum. Note the good agreement between these independent measurements of the pulse. Note also the slope of the CC SD FROG trace, which is indicative of slight chirp in the pulse. Of course, such a slope does not occur in SHG FROG traces.

We also tested the CC PG FROG technique. A measured CC PG FROG trace (of an attenuated amplified pulse train with ~ 100 nJ per pulse) is shown in Fig. 8. The relative rms error between the measured and retrieved CC PG FROG traces is 0.006, which indicates a very accurate measurement [9], [10]. In order to check this measurement, we also made a type-II CC SD FROG measurement, again using the same apparatus. The CC SD FROG trace is shown in Fig. 9. The relative rms error between the measured and retrieved CC SD FROG traces is 0.015, in agreement with the approximate noise in the measured trace. The retrieved intensities and phases are shown in Fig. 10, where we have used the standard PG FROG and SD FROG algorithms to retrieve the pulses from their traces, as required. Note the excellent agreement.

VI. CONCLUSION

Both of these techniques appear to be ideal for measuring pulses from Ti:sapphire lasers. While CC FROG is not quite as sensitive as SHG FROG and requires more care to set up than SHG FROG due to scattered input-beam light at the same wavelength as the signal, it is sufficiently sensitive for routine oscillator measurements that may require intuitive traces and freedom from direction-of-time ambiguity. We believe that, of the two methods, CC SD FROG is probably to be preferred for routine applications. This is because it lacks the slight polarizer-leakage background present in CC PG FROG, which limits the sensitivity of CC PG FROG to pulse energies that yield more than about 10^{-4} nonlinear-optical efficiency. In addition, CC SD FROG also avoids propagation through the usually thick polarizers, which can distort the pulse. Also, it is less expensive to implement, as any SHG FROG or SD FROG apparatus can be simply modified to produce a CC SD FROG device simply by changing beam angles. And, consequently, any SHG or SD autocorrelator and spectrometer can be easily modified to produce a CC SD FROG device.

Additional cascaded second-order nonlinear-optical beam geometries are also possible. For example, it is also possible to use fully phase-matched three-beam or two-crystal arrangements. But, at this time, their advantages do not appear to justify their additional complexity.

In conclusion, we have developed the first method that can rigorously measure the intensity and phase of unamplified ultrashort pulses and that yields unambiguous measurements and intuitive, familiar FROG traces.

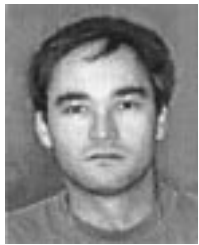
REFERENCES

- [1] D. J. Kane and R. Trebino, "Single-shot measurement of the intensity and phase of an arbitrary ultrashort pulse by using frequency-resolved optical gating," *Opt. Lett.*, vol. 18, no. 10, p. 823, 1993.
- [2] K. W. DeLong, R. Trebino, and D. J. Kane, "Comparison of ultrashort-pulse frequency-resolved-optical-gating traces for three common beam geometries," *J. Opt. Soc. Amer. B*, vol. 11, no. 9, p. 1595, 1994.
- [3] K. W. DeLong, R. Trebino, J. Hunter, and W. E. White, "Frequency-resolved optical gating with the use of second-harmonic generation," *J. Opt. Soc. Amer. B*, vol. 11, no. 11, p. 2206, 1994.
- [4] K. W. DeLong, D. N. Fittinghoff, R. Trebino, B. Kohler, and K. Wilson, "Pulse retrieval in frequency-resolved optical gating based on the method of generalized projections," *Opt. Lett.*, vol. 19, no. 24, p. 2152, 1994.
- [5] T. Tsang, M. A. Krumbügel, K. W. DeLong, D. N. Fittinghoff, and R. Trebino, "Frequency-resolved optical-gating measurements of ultrashort pulses using surface third-harmonic generation," *Opt. Lett.*, vol. 21, no. 17, p. 1381, 1996.
- [6] R. Danielius, A. Dubietis, and A. Piskarskas, "Transformation of pulse characteristics via cascaded second-order effects in an optical parametric amplifier," *Opt. Commun.*, vol. 133, p. 277, 1997.
- [7] M. A. Krumbügel, J. N. Sweetser, D. N. Fittinghoff, K. W. DeLong, and R. Trebino, "Ultrastable optical switching by use of fully phase-matched cascaded second-order nonlinearities in a polarization-gate geometry," *Opt. Lett.*, vol. 22, no. 4, p. 245, 1997.
- [8] J. N. Sweetser, M. A. Krumbügel, and R. Trebino, "Amplified ultrastable optical switching by cascaded second-order nonlinearities in a polarization-gate geometry," *Opt. Commun.*, vol. 142, p. 269, 1997.
- [9] K. W. DeLong, D. N. Fittinghoff, and R. Trebino, "Practical issues in ultrashort-laser-pulse measurement using frequency-resolved optical gating," *IEEE J. Quantum Electron.*, vol. 32, pp. 1253–1264, 1996.
- [10] D. N. Fittinghoff, K. W. DeLong, R. Trebino, and C. L. Ladera, "Noise sensitivity in frequency-resolved-optical-gating measurements of ultrashort pulses," *J. Opt. Soc. Amer. B*, vol. 12, pp. 1955–1967, 1995.



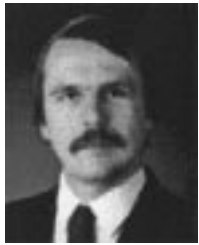
Alfred Kwok received the B.A. degree in physics and computer science from the University of California, Santa Cruz, in 1986, and the Ph.D. degree in applied physics from Yale University, New Haven, CT, in 1993.

His thesis research involved the study of interaction of lasing and stimulated Raman scattering in microdroplets. From 1993 to 1996, he was a Research Associate at the Free Electron Laser Center and the Chemistry Department at Stanford University, Palo Alto, CA, where he studied the ultrafast vibrational relaxation of glass-forming liquids and proteins, and performed the first multilevel vibrational echo-beat experiment. He is currently teaching at Franklin and Marshall College, Lancaster, PA. He tries to stay in touch with the ultrafast community and spent the summer of 1997 FROGging with R. Trebino's group at Sandia National Laboratories.



Leonard E. Jusinski born in Oakland, CA, on August 12, 1955. He received the B.S. degree in physics from the University of San Francisco, San Francisco, CA, in 1977.

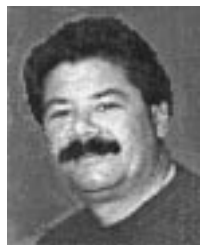
Also in 1977, he received his commission as a science officer of the U.S. Air Force, serving active duty at the Air Force Weapons Laboratory (now Phillips Laboratory), Kirtland AFB, Albuquerque, NM. Before joining Sandia National Laboratories, Livermore, CA, in June 1996, he was a member of the Technical Staff of the Molecular Physics Department at SRI International, Menlo Park, CA, where he coauthored over 50 publications in the fields of chemical kinetics and nonlinear optics.



Marco A. Krumbügel received the Diplom in physics and the Dr. rer. nat. degree from the Technical University of Berlin, Berlin, Germany, in 1990 and 1993, respectively.

His thesis research involved numerical simulations and interferometric microwave measurements of the diffraction near fields behind phase objects. Since 1995, he has held a Feodor Lynen Fellowship of the Alexander von Humboldt Foundation working in collaboration with Dr. R. Trebino from Sandia National Laboratories and Prof. A. E. Siegman from Stanford University to retrieve ultrashort-laser pulses using FROG and an artificial neural network.

Dr. Krumbügel is member of the Optical Society of America, the Deutsche Physikalische Gesellschaft, and the Deutsche Gesellschaft für angewandte Optik.



John N. Sweetser received the B.S. degree in applied and engineering physics and the M.Eng. degree in electrical engineering from Cornell University, Ithaca, NY, in 1984 and 1986, respectively, and the Ph.D. degree in optics from the University of Rochester, Rochester, NY, in 1994.

His thesis research involved the study of coherent effects in the propagation of ultrashort-laser pulses in resonant molecular systems and the development of a novel femtosecond laser amplifier. He is currently with Sandia National Laboratories,

Livermore, CA, where he is developing techniques for linear and nonlinear optical spectroscopy for gas-phase diagnostics. His other interests include ultrashort pulse measurement and applications and optical switching.



David N. Fittinghoff received the B.S. degree in physics from the University of California, Davis, in 1985 and the M.S. and Ph.D. degrees in engineering applied science from the University of California, Davis/Livermore, in 1989 and 1993, respectively.

He is currently a Researcher with the Institute for Nonlinear Science at the University of California, San Diego. His research has covered strong-field ionization of atoms, ultrashort pulse measurement including frequency-resolved optical gating, two-photon confocal microscopy, and the development

of CPA systems.

Dr. Fittinghoff is a member of the Optical Society of America and the American Physical Society.

Rick Trebino, for a biography, see this issue, p. 158.